*Article*

# Too Persistent to Resist: Aromaticity in 16e Osmapentalene Radicals Survives Regardless of Redox

Shijie Pan [1], Jun Yan [2], Weitang Li [2], Zhigang Shuai [2] and Jun Zhu [2,*]

[1] State Key Laboratory of Physical Chemistry of Solid Surfaces, Fujian Provincial Key Laboratory of Theoretical and Computational Chemistry, Department of Chemistry, College of Chemistry and Chemical Engineering, Xiamen University, Xiamen 361005, China
[2] School of Science and Engineering, The Chinese University of Hong Kong, Shenzhen 518172, China
* Correspondence: jun.zhu@cuhk.edu.cn

**Abstract:** As one of the most important concepts in organic chemistry, aromaticity has attracted considerable attention from both theoretical and experimental chemists. Limited by the traditional rules (Hückel's rules and Baird's rules), species can only achieve aromaticity in a single state ($S_0$ or $T_1$) in most cases. In 2018, our group first reported 16 electron osmapentalene that showed aromaticity in both the $S_0$ and $T_1$ states, which is defined as adaptive aromaticity. In recent years, although adaptive aromatic compounds have been expanded, the adaptive aromatics containing metal-centered radical has not been reported. Here, we carry out density functional theory calculations to explore the aromaticity of the corresponding radicals based on osmapentalyne and osmapentalenes in their $S_0$ states. It is found that the corresponding radicals of adaptive aromatic osmapentalene exhibit aromaticity regardless of the radicals formed by oxidation or reduction, supported by a series of aromaticity indices including ΔBL, NICS, AICD, EDDB, and ELF. In contrast, for the nonaromatic or antiaromatic compound in the $T_1$ state, only its cationic radical shows aromaticity. Furthermore, the spin density localization on the metal center is the key factor for the radicals to achieve aromaticity.
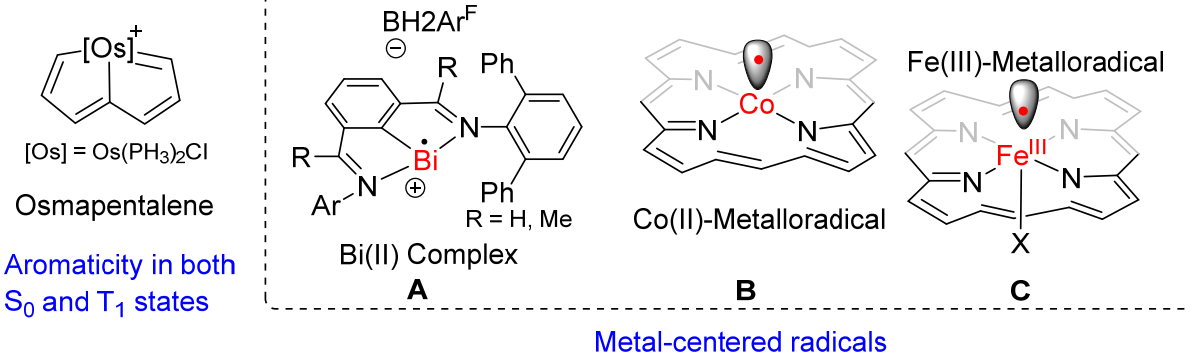
**Keywords:** aromaticity; metal-centered radical; DFT calculation
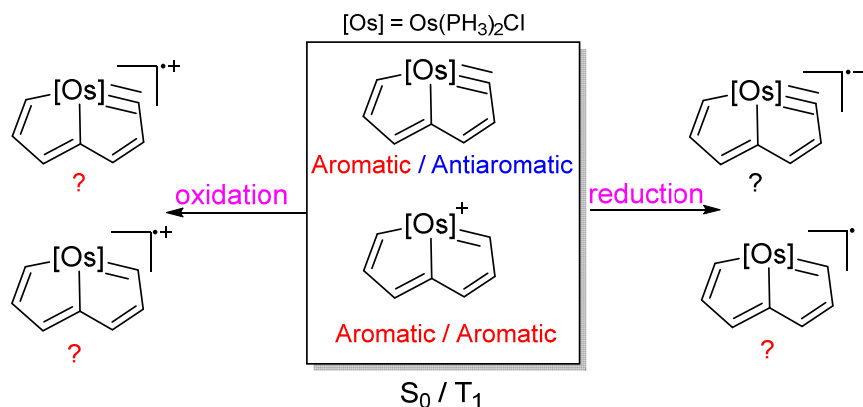
## 1. Introduction

The concept of aromaticity is of increasing interest to both experimental and theoretical chemists. In 1931, Erich Hückel studied the molecular orbital theory of π-conjugated hydrocarbons and proposed the classical [4n + 2] rule for aromaticity [1]. In the 1960s, Dewar gave an interpretation of Hückel's theory [2]. In addition, Heilbronner [3] and Zimmerman [4,5] proposed and extended the concept of Möbius aromaticity. Dating back to 1979, Thorn and Hoffmann first predicted the existence of metalla-aromatics [6]. Three years later, Roper and co-workers synthesized the inaugural metallabenzene [7]. Subsequently, a series of metalla-aromatics were synthesized, encompassing metallabenzene [8–14], metallabenzyne [15–17], metallanaphthalyne [18–20], metallapentalyne [21–23], metallapentalene [24,25], and certain heteroatom-containing metallacycles such as metallafuran and its derivatives [26–28]. In 2013, Xia and co-workers reported the synthesis of aromatic metallapentalyne [29], which was a stark contrast to classical organic chemistry's antiaromatic pentalyne counterpart. According to Hückel's and Baird's rules [1,30], cyclic conjugated species with 4n + 2 π-electrons have aromaticity in their singlet electronic ground state ($S_0$) whereas they are antiaromatic in their lowest triplet state ($T_1$); conversely, species with 4n π-electrons are deemed antiaromatic in the $S_0$ state but show aromaticity in the $T_1$ state. Limited by

the two rules, species can only achieve aromaticity in a single state ($S_0$ or $T_1$). Up until 2018, our group conducted density functional theory calculations on osmapentalyne and osmapentalenes, unveiling an unprecedented example showcasing adaptive aromaticity (compound shows aromaticity in both the $S_0$ and $T_1$ states) [31], subsequently extending this phenomenon to ruthenacycles alongside other species (Scheme 1a) [32–36]. In addition, as one of the novel types among nonclassical aromaticity, metalloaromaticity gradually expanded the exploration from relatively small ring systems to macrocyclic metallaaromatic molecules both theoretically and experimentally [37–40]. Moreover, the concept of aromaticity has also been applied to catalysis [41,42].



**Scheme 1.** (**a**) Previous work on aromaticity and metal-centered radicals. (**b**) Aromaticity analysis of radicals in this work.

As one of the most important active substances in organic chemistry, free radicals play an important role in the synthesis of complex natural products [43]. More attention has been paid to radicals in organic systems, especially carbon-centered radicals [44–51]. The study of heteroatom-centered radicals has also been steadily advancing [52,53], and it was surprising to find that the aromaticity in boron clusters survives radical structural changes [54]. There is also a lot of research on metal-centered radicals [55–59], which are used in a variety of reactions and helpful to the drug development [60]. In 2023, Cornella and co-workers reported the synthesis and characterization of two organobismuth(II) compounds (Scheme 1a Compound **A**), which were proven as metal-centered radicals with little delocalization onto the ligands by experimental data and DFT calculations [61]. Recently, Zhang and co-workers [62–64] combined experimental and theoretical studies to reveal stable metalloradicals (Compounds **B** and **C** in Scheme 1a) in the cyclopropanation reaction of asymmetric olefins and proposed a potential stepwise radical mechanism. Specifically, a cobalt-based metal radical catalyzed realization of the radical chemoselective intermolecular amination of the C-H bond at an allyl position effectively advanced the radical approach

in the design of stereoselective organic synthesis and showed the importance of metallo-radicals. In addition, metal radicals have also been used in the supramolecular field to form highly luminescent metallosupramolecular radical cages [65]. Inspired by the role of metal-centered radicals and our continuing interest in aromaticity, here we explore the aromaticity of the corresponding radicals based on osmapentalynes and osmapentalenes in the $T_1$ state, respectively, forming by oxidation and reduction (Scheme 1b). We carry out density functional theory (DFT) calculations on the metal-centered radicals to investigate whether the corresponding radicals based on adaptive aromatic compound still hold aromaticity in order to extend the scope of this novel family.

## 2. Methods

All the DFT calculations were carried out with Gaussian 16 software package [66]. Geometric optimizations, together with frequency calculations, were performed at the B3LYP level of theory. The 6-311++G (d, p) basis set was employed for C, H, and O atoms. For P, Cl and Os atoms, the pseudopotential basis set LANL2DZ was used, with polarization functions for P ($\zeta(d) = 0.340$), Cl ($\zeta(d) = 0.514$), and Os ($\zeta(f) = 0.886$) [67,68]. Visualizations of structures are achieved by the CYLview program (version 1.0) [69]. NICS calculations [70] were carried out at (U)B3LYP-GIAO/def2-TZVP-level. Frequency calculations were performed to confirm that all optimized structures were energy minima. NICS(1)$_{zz}$ values were obtained by placing ghost atoms at 1Å above/below the ring centers at the (U)B3LYP/def2-TZVP-level of theory. The electron density of delocalized bond (EDDB) analysis was carried out with RunEDDB [71,72]. EDDB was employed at the B3LYP/def2-TZVP-level. The anisotropy of the induced current density (AICD) plots was obtained using the AICD 2.0 program. The topological analysis implemented by Multiwfn (3.8 dev.) [73] is used to accurately locate the ELF$_\pi$ bifurcation points by searching the critical points in the sphere and taking each nucleus in the molecule as the center of the sphere in turn.

## 3. Results and Discussion

### 3.1. The Geometries of the Corresponding Radicals from Complexes **1** to **3**

Due to the different Gaussian versions used (the previous work was carried out with Gaussian 03), we initially recalculated the previous studies on model complexes **1–3** (Figure S1) for better comparative analysis. Based on the various analysis, all these three complexes in the $S_0$ state (**1-S$_0$**, **2-S$_0$**, and **3-S$_0$**) and complex **2** in the $T_1$ state (**2-T$_1$**) are aromatic, which indicates that the complex **2** has adaptive aromaticity, in line with our previous findings [31]. Similarly, we examined their corresponding radicals, which are obtained by oxidation (complexes **1-rad.1**, **2-rad.1** and **3-rad.1**) and reduction (complexes **1-rad.2**, **2-rad.2** and **3-rad.2**) by removing and adding one electron, respectively. As shown in Figure 1, the C–C bond lengths of these metal radicals are in the range of 1.358–1.448 Å, which are between the carbon–carbon double bond (1.333 Å in $CH_2=CH_2$) and the single bond (1.527 Å in $CH_3–CH_3$) calculated at the same level of theory. The bond length alternations ($\Delta$BL) of the three radical cations (**1-rad.1**, **2-rad.1** and **3-rad.1**) are 0.035, 0.042, 0.028Å, which indicate their aromaticity. On the contrary, the bond length alternations ($\Delta$BL) of the radicals obtained by reduction are quite different. Only the complex **2-rad.2** has a relatively small bond length alternation (0.012Å), showing the potential of aromaticity. By the way, the relative energies of $T_1$ and $D_0$ with respect to the $S_0$ state are shown in Table 1.

**Table 1.** The relative energy (kcal/mol) of $T_1$ and $D_0$ states with respect to the $S_0$ state. The values of $\Delta E_{S-T}$ are equal to $E_S - E_T$, standing for the relative energy between the $S_0$ state and the $T_1$ state. Similarly, the values of $\Delta E_{S-D}$ show the relative energy of radicals with respect to the $S_0$ state (D1: **rad.1**; D2: **rad.2**).

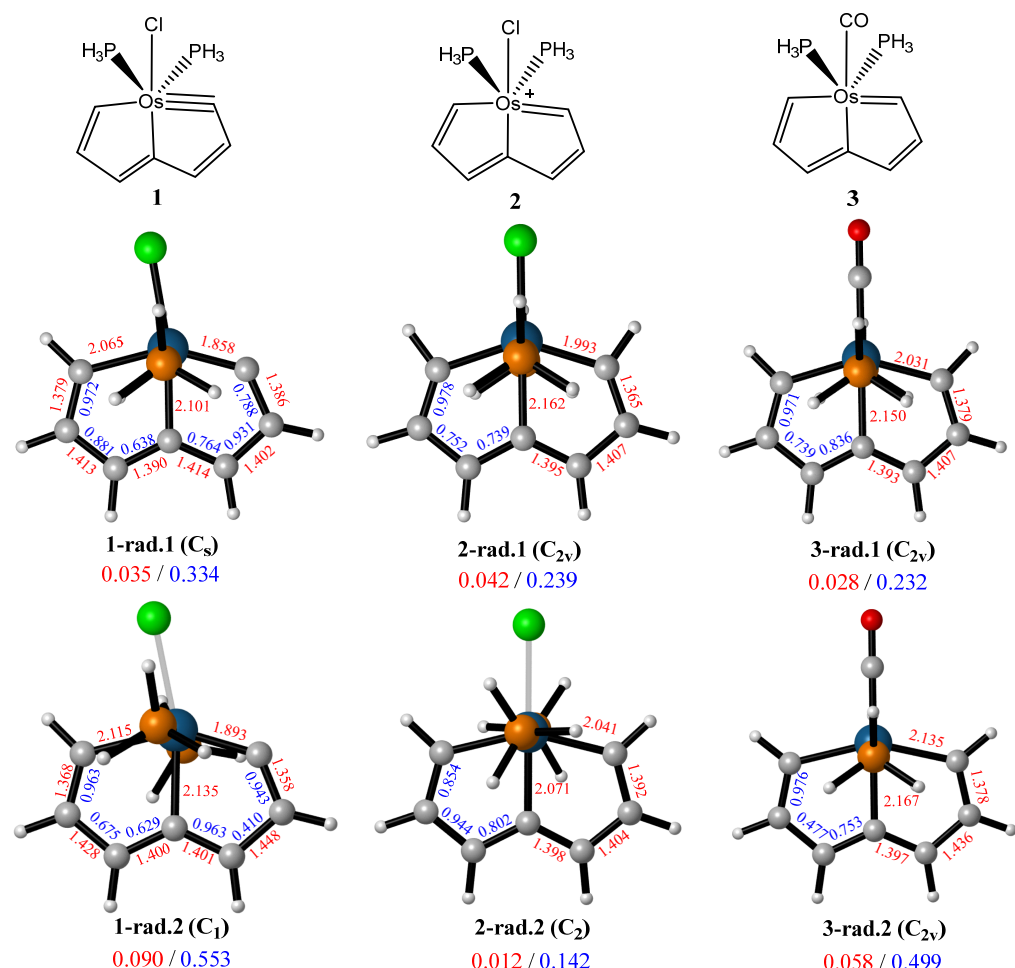| Compounds | $\Delta E_{S-T}$ | $\Delta E_{S-D1}$ | $\Delta E_{S-D2}$ |
|:---:|:---:|:---:|:---:|
| **1** | −44.2 | −168.8 | 23.6 |
| **2** | −21.6 | −269.3 | 140.2 |
| **3** | −36.0 | −155.1 | 24.0 |



**Figure 1.** The structures of radicals obtained from complexes **1**–**3** by oxidation and reduction. The bond lengths (Å, red) and $ELF_\pi$ bifurcation values (blue) are annotated along the bonds. The bond length alternations [$\Delta BL$(Å), in red] and $\Delta BV(ELF_\pi)$ values (in blue) of the ring excluding the C-Os-C fragment are annotated below the geometry structures separated by a slash ("/").

### 3.2. Aromaticity Analyses Based on Magnetic Properties

To further assess the (anti-)aromaticity of these complexes, we conducted the nucleus-independent chemical shift (NICS) calculations in their different states. NICS, proposed by Schleyer and co-workers has emerged as one of the most widely accepted criteria for determining aromaticity [74–76]. It is derived from computing the magnetic shielding effect of virtual atoms at any point on the ring (typically at the ring center for σ-aromaticity or 1 Å above the ring center for π-aromaticity). Commonly, significantly negative NICS values indicate aromaticity whereas positive NICS ones suggest antiaromaticity. The two-dimensional NICS grids are capable to show the magnetic shielding in aromatic rings while de-shielding in antiaromatic rings [77,78]. A value close to zero can be considered non-

aromatic. In comparison with NICS(0)$_{zz}$, the NICS(1)$_{zz}$ value is used here as it was reported to be more suitable in evaluating $\pi$ aromaticity [79]. Surprisingly, the corresponding radical cations (**1-rad.1**, **2-rad.1**, **3-rad.1**) all show aromaticity (Figure 2) within significantly negative (shielded) NICS(1)$_{zz}$ values (ranging from $-21.0$ ppm to $-28.2$ ppm), regardless of the aromaticity of the T$_1$ state itself. However, when the corresponding radicals are obtained by reduction, their aromaticity has different characteristics. Only the radical from compound **2** (**2-rad.2**) remains aromatic within significant negative NICS(1)$_{zz}$ values ($-24.5$ ppm), whereas the corresponding radical anions, **1-rad.2** (0.6/4.3 ppm) and **3-rad.2** (0.6 ppm), exhibit non-aromaticity.
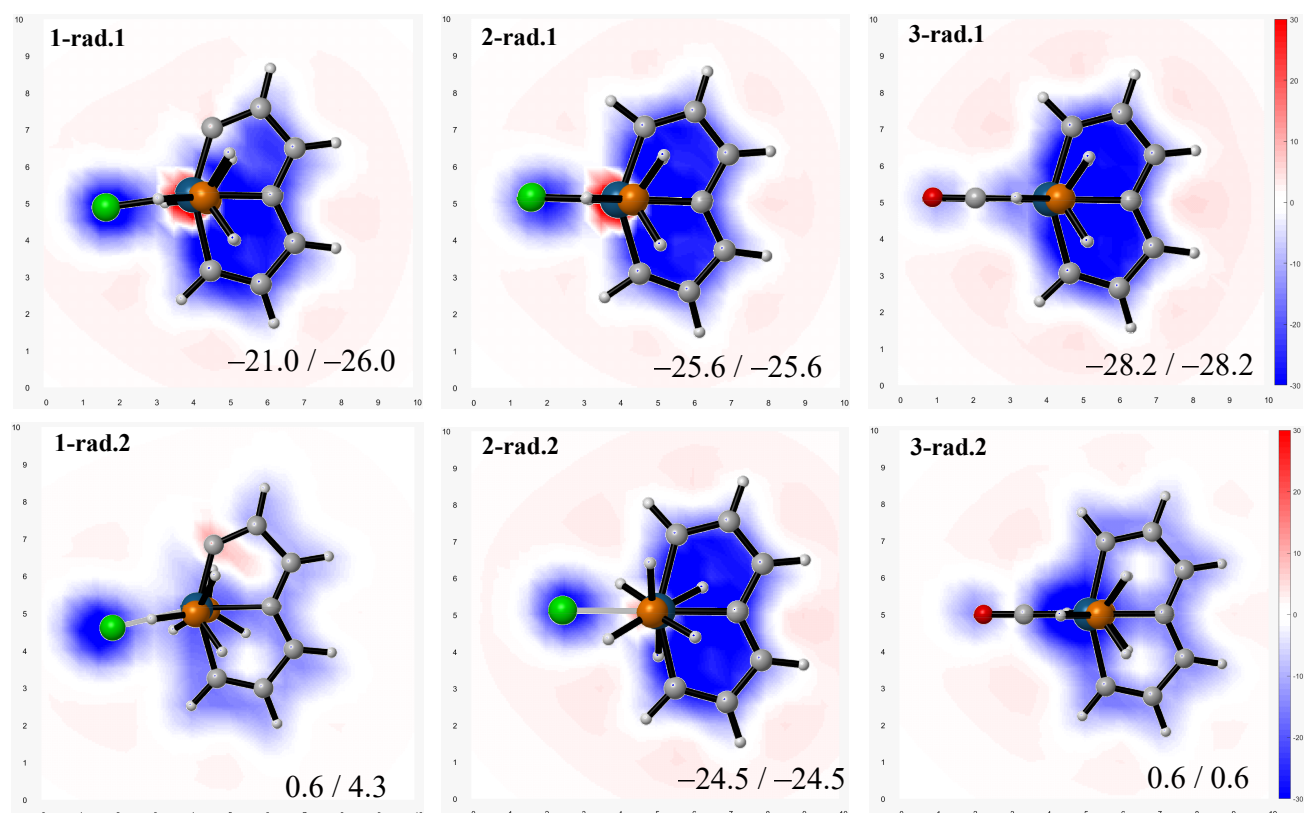


**Figure 2.** NICS(1)$_{zz}$ grids for metallacyclopropene rings in corresponding radicals of complexes **1–3** obtained by oxidation (rad.1) and reduction (rad.2), respectively (values (ppm) provided on the bottom of each graph).

To further support the (anti-)aromaticity of these complexes, anisotropy of the induced current density (AICD) analyses was performed to examine the magnetic anisotropy, which has been proven to be a general method for visualizing delocalized electrons [80,81]. Generally, the clockwise ring current indicates aromaticity in the fused rings, and the anti-clockwise ring suggests anti-aromaticity. Clockwise currents along the perimeter of the fused rings in **1-rad.1**, **2-rad.1**, **3-rad.1,** and **2-rad.2** indicate aromaticity, consistent with the NICS grids. In sharp contrast, the ring currents in **1-rad.2** and **3-rad.2** are tiny and disordered, characteristic of non-aromaticity (Figure 3). High-resolution plots are provided in the Supporting Information (Figures S4–S15).
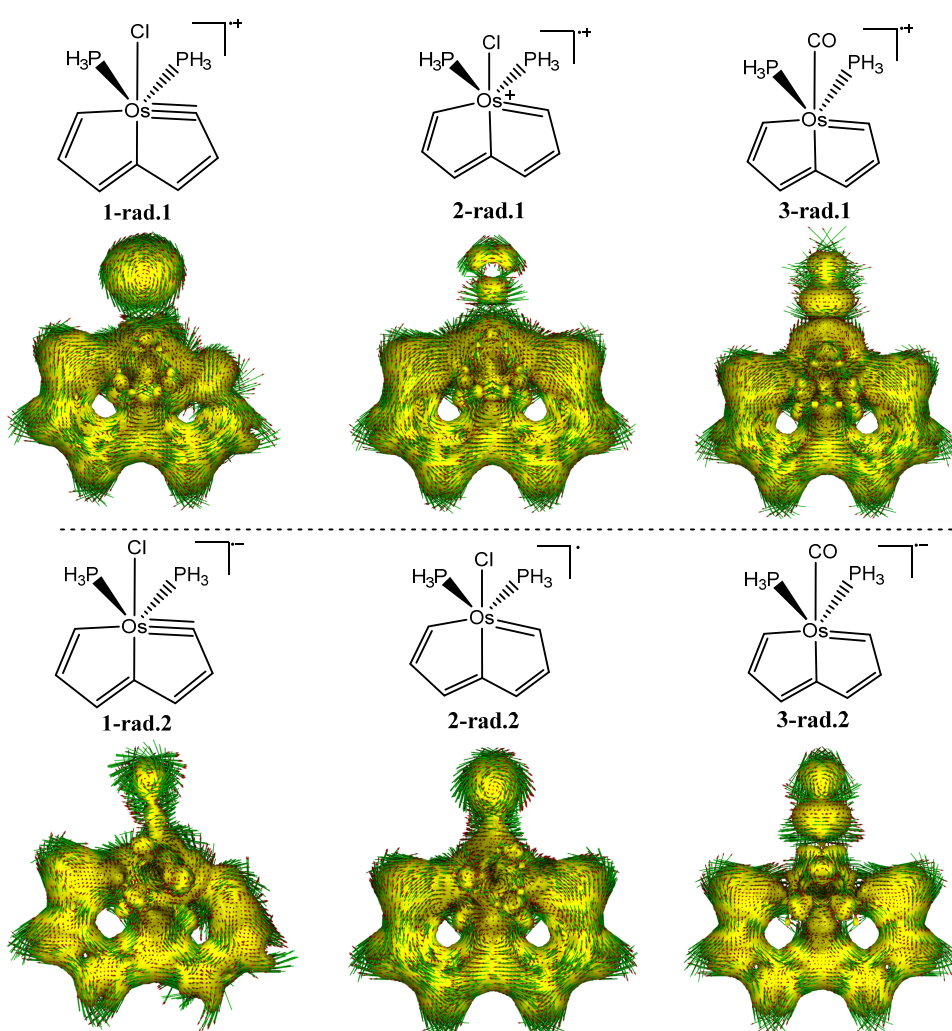
**Figure 3.** AICD plots of the corresponding radicals of complexes **1–3**. The molecular planes are placed perpendicular to the magnetic field vector. Small green arrows are computed current density vectors. The isovalue for the surfaces is 0.030 a.u. The paratropic/diatropic ring currents indicate antiaromaticity and aromaticity, respectively.

*3.3. Electron Density of Delocalized Bonds (EDDB) Analysis*

The essence of aromaticity is the delocalization of electrons, and EDDB, proposed by Szczepanik and co-workers in 2014 [71], exhibits an advantage in evaluating the delocalized electrons quantitatively. It can be used to efficiently achieve the separation of σ and π contributions, and provides contribution of delocalized electrons from the specific fragments. The π electrons of the 8MR play an important role in aromaticity and the EDDB method is powerful in quantifying the delocalized electrons. Therefore, the π-EDDB_F method for the complex 8MR fragment was used in the aromaticity analysis (Figure 4). For a given system, the relatively larger EDDB values indicate more delocalized electrons and stronger aromaticity. The π-EDDB_F values of the radical cations (**1-rad.1**, **2-rad.1** and **3-rad.1**) are relatively large (ranging from 4.83 e to 5.31 e), indicating their aromaticity, whereas among the radicals formed by reduction, only the corresponding radical of compound **2**, within adaptive aromaticity, has a large π-EDDB_F value (5.87 e) and shows its aromaticity. According to the π-EDDB values of the 8MR, the results are in line with that from NICS and AICD analyses. In addition, we selected the key natural orbitals for bond delocalization (NOBDs) with π-contributions and provided them in Figures S16–S18.
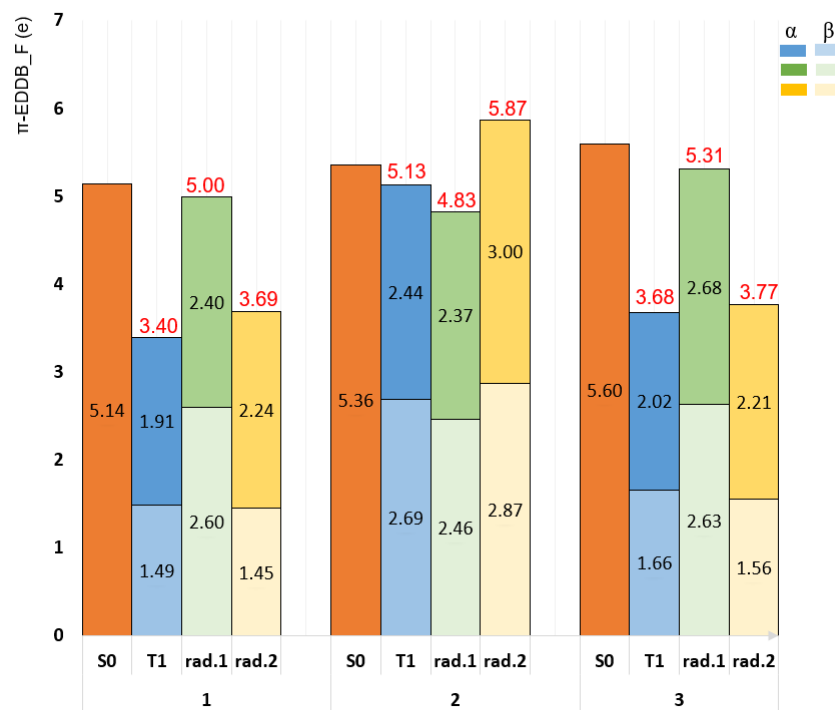
**Figure 4.** $\pi$-EDDBF(r)_F of 8MR fragment plots of complexes **1–3** in the $S_0$, $T_1$ states and corresponding radicals, respectively. The numbers in red refer to the delocalized electrons of different states.

### 3.4. Aromaticity Analyses Based on Electron Localization Function

For a better determination of aromaticity, we also manipulated topological analysis of electron localization function (ELF) which was used to assess the (anti-)aromaticity of systems by linking the properties of molecular electronic structure. It is worth noting that $ELF_\pi$ ($\pi$-contribution to ELF) performs well in measuring (anti)aromaticity. A small span of $ELF_\pi$ bifurcation values ($\Delta BV(ELF_\pi)$) for C-C bonds is an indicator of aromaticity, the $\Delta BV(ELF_\pi)$s (range from 0.232 to 0.334, as shown in Figure 1) in the radicals **1-rad.1**, **2-rad.1** and **3-rad.1** are close to that of the compounds (0.108–0.235), which were proved to be aromatic by our previous work [31], indicating the better electron delocalization and their aromaticity. In addition, the $\Delta BV(ELF_\pi)$ of the radical **2-rad.2** is small (0.142), indicating its aromaticity. In contrast, the $\Delta BV(ELF_\pi)$ in antiaromatic compound **1-$T_1$** (0.721) is more than six times of that in aromatic **1-$S_0$** (0.108), consisting with our previous work (Figure S1) [31]. The intermediate $\Delta BV(ELF_\pi)$ (0.476–0.553) of **3-$T_1$**, **1-rad.2** and **3-rad.2** indicate their non-aromaticity. All these results are in line with those from NICS, AICD, and EDDB analyses.

### 3.5. Aromaticity Analyses Based on Frontier Molecular Orbitals and Spin Populations

To explore the origin for the aromaticity of the corresponding radicals from compound **2**, obtained by oxidation or reduction, we analyzed their frontier molecular orbitals. As shown in Figure 5, the highest singly occupied molecular orbitals (HSOMO) of the radical cations (**1-rad.1**, **2-rad.1** and **3-rad.1**) obtained by oxidation are extremely similar to the HSOMO-1 of the parent complexes in the $T_1$ state. In the case of compound **2**, the HSOMO of **2-rad.1** exhibits an out-of-plane orientation. When compared to the HSOMO-1 of **2-$T_1$**, it becomes evident that this out-of-plane orientation contributes more significantly to its aromaticity. As for radical cations **1-rad.1** and **3-rad.1**, they will not be affected by the contribution to out-of-plane antiaromaticity, thus they could keep their aromaticity. Meanwhile, the HSOMO of **1-rad.1** shows a slight clockwise current, which indicates that it contributes a slight contribution for the aromaticity. It is interesting that the radicals obtained by

reduction perform different aromaticity and only the radical **2-rad.2** keeps aromaticity whereas the radical anions (**1-rad.2** and **3-rad.2**) become nonaromatic. Focusing on the radicals **1-rad.2**, **2-rad.2** and **3-rad.2**, their HSOMOs are similar to the HSOMOs of parent complexes in the $T_1$ state. For complex **2**, the HSOMO of the triplet ($T_1$) state is oriented in-plane, thereby allowing us to disregard its contribution to out-of-plane aromaticity, in line with our previous work [31]. Similarly, in complex **2-rad.2**, the HSOMO also exhibits an in-plane orientation, and this orientation does not reverse its aromaticity. However, the aromaticity change in radical anions **1-rad.2** and **3-rad.2** could contribute to the newly generated significantly paratropic ring current of HSOMOs. All these qualitative analyses are also supported by AICD calculations on these key frontier molecular orbitals (Figure 5).
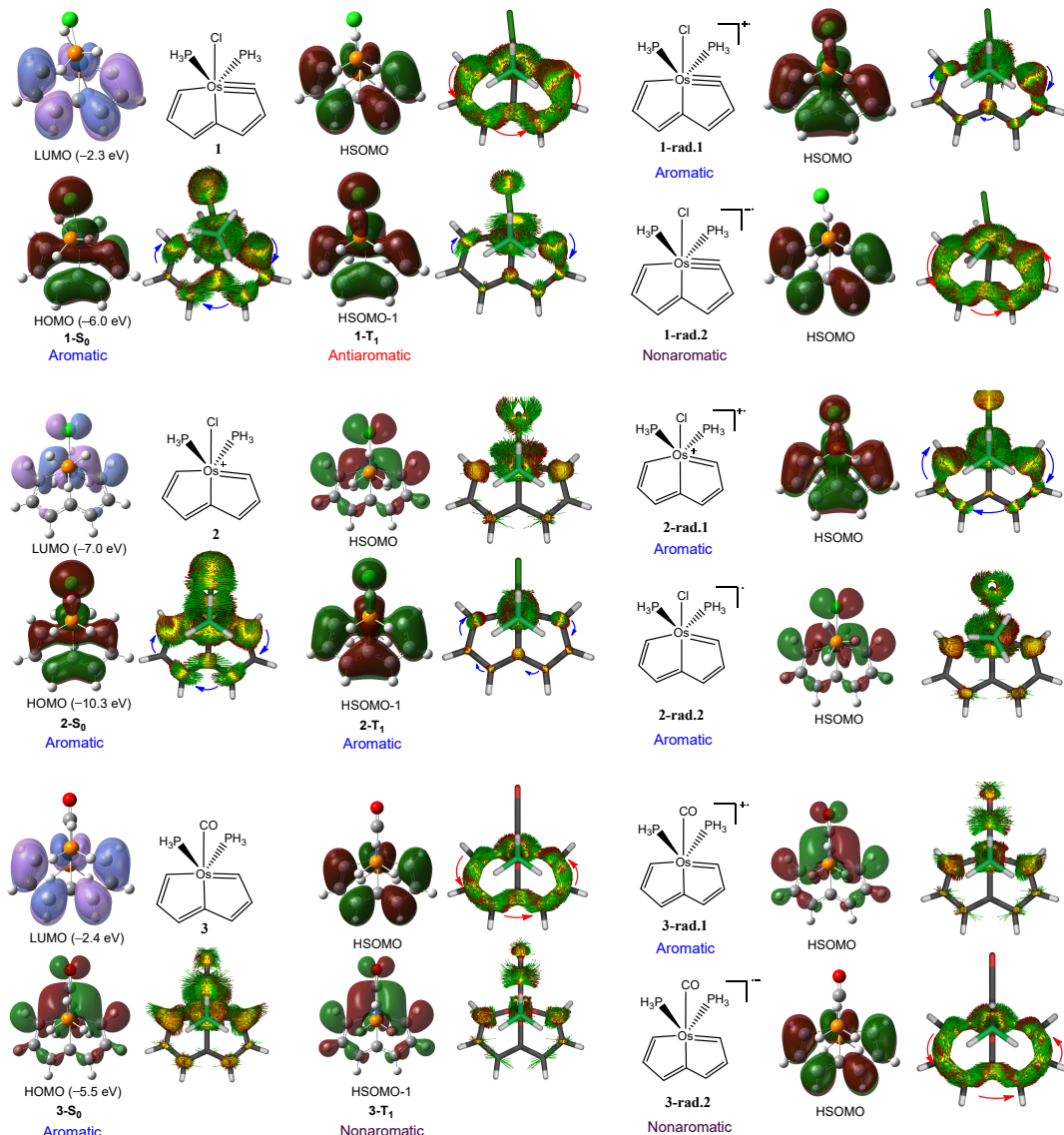


**Figure 5.** AICD plots for individual molecular orbitals. Although all the listed MOs possess $\pi$ character, the "$\pi$ orbitals" we discussed in this study only refer to those anti-symmetric to the molecular plane. The isovalues for MO and AICD surfaces are 0.02 and 0.024 a.u., respectively. High-resolution plots are provided in the Supporting Information (Figures S19–S33).

The studies have demonstrated that the localized spin density on metal center is beneficial to achieve aromaticity for complexes [31,35,36]. In line with the previous findings, aromatic systems (compounds **1-rad.1**, **2-$T_1$**, **2-rad.1**, **2-rad.2** and **3-rad.1**) display localized spin density on the metal center, whereas other anti(non-)aromatic complexes have spin

density distributed mainly on the carbon rings. As shown in Figure 6, the spin populations on the osmium center of complexes **1-rad.1**, **2-T$_1$**, **2-rad.1**, **2-rad.2** and **3-rad.1** are large (45.12–68.41%). In contrast, the spin population on the seven carbon atoms of the eight-membered ring (R$_{7C}$) in these complexes are relatively small. Conversely, the atomic spin population in the nonaromatic radical anions **1-rad.2** and **3-rad.2** are mostly distributed on the carbon atoms rather than the metal center, similar to the **1-T$_1$** and **3-T$_1$**. In summary, the spin density contributed on the metal center plays a crucial rule in their aromaticity.
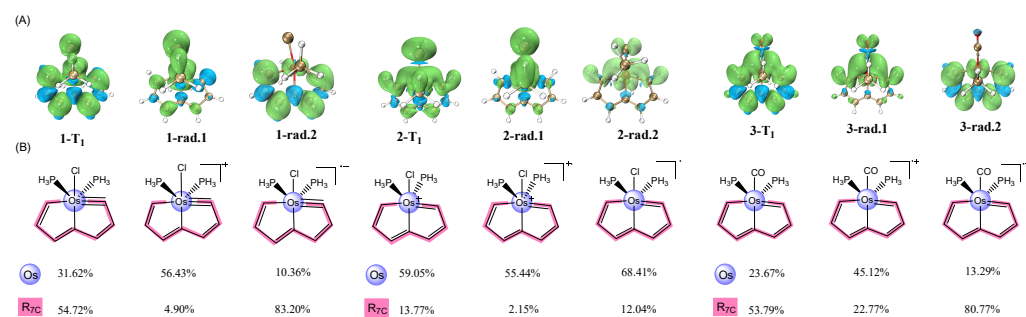


**Figure 6.** Spin density analysis (**A**) and spin populations (**B**) of complexes **1**–**3** in T$_1$ state and corresponding radicals.

## 4. Conclusions

We performed DFT calculations on the osmapentalyne, as well as osmapentalene complexes and their corresponding radicals. It was found that the corresponding radicals of adaptive aromatic complex **2** retain aromaticity regardless of the radicals formed by oxidation or reduction, supported by various aromaticity indices including ΔBL, NICS, AICD, EDDB and ELF. It is necessary to try as many aromatic indices as possible because using a single index is unilateral and may lead to inconsistent judgements [82,83]. The localization of spin electrons on the metal center could be regarded as one of the key reasons to achieve aromaticity. All these findings not only deepen the understanding of the concept of aromaticity, but also help the development of radical chemistry.

HSOMO-1 of **3-T$_1$**; Figure S32: AICD plot of the HSOMO of **3-rad.1**; Figure S33: AICD plot of the HSOMO of **3-rad.2**; Cartesian coordinates of all the species.

**Author Contributions:** J.Z. conceived and supervised the project. S.P., J.Y., W.L. and Z.S. performed the theoretical calculation. S.P. drafted the manuscript and J.Z. revised it. All authors have contributed to the final version of the manuscript. All authors have read and agreed to the published version of the manuscript.

**Data Availability Statement:** Data are contained within the article or the Supplementary Materials.

**Conflicts of Interest:** The authors declare no conflicts of interest.

# References

1.  Hückel, E. Quantentheoretische Beiträge zum Benzolproblem. *Z. Phys.* **1931**, *70*, 204–286. [CrossRef]
2.  Dewar, M.J.S. A molecular orbital theory of organic chemistry-VIII: Aromaticity and electrocyclic reactions. *Tetrahedron* **1966**, *22*, 75–92. [CrossRef]
3.  Heilbronner, E. Hückel molecular orbitals of Möbius-type conformations of annulenes. *Tetrahedron Lett.* **1964**, *5*, 1923–1928. [CrossRef]
4.  Zimmerman, H.E. On molecular orbital correlation diagrams, the occurrence of Möbius systems in cyclization reactions, and factors controlling ground-and excited-state reactions. I. *J. Am. Chem. Soc.* **1966**, *88*, 1564–1565. [CrossRef]
5.  Zimmerman, H.E. Möbius-Hückel concept in organic chemistry. Application of organic molecules and reactions. *Acc. Chem. Res.* **1971**, *4*, 272–280. [CrossRef]
6.  Thorn, D.L.; Hoffmann, R. Delocalization in metallocycles. *Nouv. J. Chem.* **1979**, *3*, 39–45.
7.  Elliott, G.P.; Roper, W.R.; Waters, J.M. Metallacyclohexatrienes or 'Metallabenzenes' Synthesis of Osmabenzene Derivatives and X-Ray Crystal-Structure of [Os(CsCHCHCHCH)(Co)(PPh$_3$)$_2$]. *J. Chem. Soc. Chem. Commun.* **1982**, *14*, 811–813. [CrossRef]
8.  Bleeke, J.R. Metallabenzenes. *Chem. Rev.* **2001**, *101*, 1205–1228. [CrossRef] [PubMed]
9.  He, G.; Xia, H.; Jia, G. Progress in the synthesis and reactivity studies of metallabenzenes. *Chin. Sci. Bull.* **2004**, *49*, 1543–1553. [CrossRef]
10. Landorf, C.W.; Haley, M.M. Recent Advances in Metallabenzene Chemistry. *Angew. Chem. Int. Ed.* **2006**, *45*, 3914–3936. [CrossRef] [PubMed]
11. Bleeke, J.R. Aromatic Iridacycles. *Acc. Chem. Res.* **2007**, *40*, 1035–1047. [CrossRef]
12. Paneque, M.; Poveda, M.L.; Rendón, N. Synthesis and Reactivity of Iridacycles Containing the Tp$^{Me2}$Ir Moiety. *Eur. J. Inorg. Chem.* **2011**, *2011*, 19–33. [CrossRef]
13. Zhu, C.; Cao, X.; Xia, H. Double Stabilization of Highly Strained Six-Membered Rings by Phosphonium and Transition Metal. *Chin. J. Org. Chem.* **2013**, *33*, 657–662. [CrossRef]
14. Cao, X.Y.; Zhao, Q.; Lin, Z.; Xia, H. The Chemistry of Aromatic Osmacycles. *Acc. Chem. Res.* **2014**, *47*, 341–354. [CrossRef] [PubMed]
15. Wen, T.B.; Zhou, Z.Y.; Jia, G. Synthesis and Characterization of a Metallabenzyne. *Angew. Chem. Int. Ed.* **2001**, *40*, 1951–1954. [CrossRef]
16. Jia, G. Recent progress in the chemistry of osmium carbyne and metallabenzyne complexes. *Coord. Chem. Rev.* **2007**, *251*, 2167–2187. [CrossRef]
17. Chen, J.; Jia, G. Recent development in the chemistry of transition metal-containing metallabenzenes and metallabenzynes. *Coord. Chem. Rev.* **2013**, *257*, 2491–2521. [CrossRef]
18. He, G.; Zhu, J.; Hung, W.Y.; Wen, T.B.; Sung HH, Y.; Williams, I.D.; Lin, Z.; Jia, G. A Metallanaphthalyne Complex from Zinc Reduction of a Vinylcarbyne Complex. *Angew. Chem. Int. Ed.* **2007**, *46*, 9065–9068. [CrossRef]
19. Zhang, M.-X.; Zhang, J.; Jin, X.; Sun, X.; Yin, J.; Hartl, F.; Liu, S.H. Diphenylamine-Substituted Osmanaphthalyne Complexes: Structural, Bonding, and Redox Properties of Unusual Donor–Bridge–Acceptor Systems. *Chem. Eur. J.* **2018**, *24*, 18998–19009. [CrossRef]
20. Zhang, M.-X.; Xu, Z.; Lu, T.; Yin, J.; Liu, S.H. A Visible-Light-Induced Strategy To Construct Osmanaphthalynes, Osmaanthracyne, and Osmaphenanthryne. *Chem. Eur. J.* **2018**, *24*, 14891–14895. [CrossRef] [PubMed]

21. Zhu, C.; Yang, Y.; Wu, J.; Luo, M.; Fan, J.; Zhu, J.; Xia, H. Five-Membered Cyclic Metal Carbyne: Synthesis of Osmapentalynes by the Reactions of Osmapentalene with Allene, Alkyne, and Alkene. *Angew. Chem. Int. Ed.* **2015**, *54*, 7189–7192. [CrossRef] [PubMed]

22. Zhuo, Q.; Lin, J.; Hua, Y.; Zhou, X.; Shao, Y.; Chen, S.; Chen, Z.; Zhu, J.; Zhang, H.; Xia, H. Multiyne chains chelating osmium via three metal-carbon σ bonds. *Nat. Commun.* **2017**, *8*, 1912. [CrossRef] [PubMed]

23. Zhu, C.; Xia, H. Carbolong Chemistry: A Story of Carbon Chain Ligands and Transition Metals. *Acc. Chem. Res.* **2018**, *51*, 1691–1700. [CrossRef]

24. Zhu, C.; Luo, M.; Zhu, Q.; Zhu, J.; Schleyer, P.v.R.; Wu, J.I.-C.; Lu, X.; Xia, H. Planar Möbius aromatic pentalenes incorporating 16 and 18 valence electron osmiums. *Nat. Commun.* **2014**, *5*, 3265. [CrossRef] [PubMed]

25. Zhu, C.; Yang, C.; Wang, Y.; Lin, G.; Yang, Y.; Wang, X.; Zhu, J.; Chen, X.; Lu, X.; Liu, G.; et al. CCCCC pentadentate chelates with planar Möbiusaromaticity and unique properties. *Sci. Adv.* **2016**, *2*, e1601031. [CrossRef]

26. Grotjahn, D.B.; Hoerter, J.M.; Hubbard, J.L. Double C-H Activation during Functionalization of Phenyl(methyl)ketene on Iridium(I) Using Alkynes. Synthesis of 1,4-Dien-3-ones. *J. Am. Chem. Soc.* **2004**, *126*, 8866–8867. [CrossRef]

27. Weller, K.J.; Filippov, I.; Briggs, P.M.; Wigley, D.E. Pyridine Degradation Intermediates as Models for Hydrodenitrogenation Catalysis: Preparation and Properties of a Metallapyridine Complex. *Organometallics* **1998**, *17*, 322–329. [CrossRef]

28. Wang, T.; Han, F.; Huang, H.; Li, J.; Zhang, H.; Zhu, J.; Lin, Z.; Xia, H. Synthesis of Aromatic Aza-metallapentalenes from Metallabenzene via Sequential Ring Contraction/Annulation. *Sci. Rep.* **2015**, *5*, 9584. [CrossRef] [PubMed]

29. Zhu, C.; Li, S.; Luo, M.; Zhou, X.; Niu, Y.; Lin, M.; Zhu, J.; Cao, Z.; Lu, X.; Wen, T.; et al. Stabilization of anti-aromatic and strained five-membered rings with a transition metal. *Nat. Chem.* **2013**, *5*, 698–703. [CrossRef]

30. Baird, N.C. Quantum Organic Photochemistry. II. Resonance and Aromaticity in the Lowest ππ* State of Cyclic Hydrocarbons. *J. Am. Chem. Soc.* **1972**, *94*, 4941–4948. [CrossRef]

31. Chen, D.; Shen, T.; An, K.; Zhu, J. Adaptive aromaticity in $S_0$ and $T_1$ states of pentalene incorporating 16 valence electron osmium. *Commun. Chem.* **2018**, *1*, 18. [CrossRef]

32. Chen, D.; Qiu, R.; Dong SZhu, J. Adaptive aromaticity in ruthenacycles. *Theor. Chem. Acc.* **2020**, *139*, 21. [CrossRef]

33. Dai, C.; Chen, D.; Zhu, J. Achieving Adaptive Aromaticity in Cyclo[10]carbon by Screening Cyclo[n]carbon (n=8-24). *Chem. Asian J.* **2020**, *15*, 2187–2191. [CrossRef] [PubMed]

34. Huang, Y.; Chen, D.; Zhu, J. Adaptive Aromaticity in Metallasilapentalynes. *Organometallics* **2021**, *40*, 899–906. [CrossRef]

35. Xu, F.; Chen, D.; Zeng, J.; Zhu, J. Osmapentalyne and Osmapentalene Complexes Containing Boron Monofluoride Ligands: Structure, Bonding and Adaptive Aromaticity. *New J. Chem.* **2021**, *45*, 15294–15302. [CrossRef]

36. Qiu, R.; Zhu, J. Adaptive Aromaticity in 16-valence-electron Metallazapentalenes. *Dalton Trans.* **2021**, *50*, 16842–16848. [CrossRef] [PubMed]

37. Wei, J.; Zhang, Y.; Chi, Y.; Liu, L.; Zhang, W.-X.; Xi, Z. Aromatic Dicupra[10]Annulenes. *J. Am. Chem. Soc.* **2016**, *138*, 60–63. [CrossRef]

38. An, K.; Shen, T.; Zhu, J. Craig-Type Möbius Aromaticity and Antiaromaticity in Dimetalla[10]Annulenes: A Metal-Induced Yin-and-Yang Pair. *Organometallics* **2017**, *36*, 3199–3204. [CrossRef]

39. Miwa, K.; Yokota, T.; Wang, Q.; Sakurai, T.; Fliegl, H.; Sundholm, D.; Shinokubo, H. Metallaantiaromaticity of 10-Platinacorrole Complexes. *J. Am. Chem. Soc.* **2024**, *146*, 1396–1402. [CrossRef] [PubMed]

40. Merino, G.; Solà, M.; Fernández, I.; Foroutan-Nejad, C.; Lazzeretti, P.; Frenking, G.; Anderson, H.L.; Sundholm, D.; Cossío, F.P.; Petrukhina, M.A.; et al. Aromaticity: Quo Vadis. *Chem. Sci.* **2023**, *14*, 5569–5576. [CrossRef] [PubMed]

41. Gonçalves, T.P.; Dutta, I.; Huang, K.-W. Aromaticity in catalysis: Metal ligand cooperation via ligand dearomatization and rearomatization. *Chem. Commun.* **2021**, *57*, 3070–3082. [CrossRef] [PubMed]

42. Gonçalves, T.P.; Huang, K.-W. Metal–Ligand Cooperative Reactivity in the (Pseudo)-Dearomatized PNx(P) Systems: The Influence of the Zwitterionic Form in Dearomatized Pincer Complexes. *J. Am. Chem. Soc.* **2017**, *139*, 13442–13449. [CrossRef] [PubMed]

43. Chatgilialoglu, C.; Studer, A. *Encyclopedia of Radicals in Chemistry, Biology and Materials*; Wiley: Chichester, UK, 2012.

44. Tang, S.; Liu, K.; Liu, C.; Lei, A. Olefinic C–H functionalization through radical alkenylation. *Chem. Soc. Rev.* **2015**, *44*, 1070. [CrossRef]

45. Hammer, S.G.; Heinrich, M.R. Carbon-Carbon Bond-Forming Reactions Involving Aryl Radicals. In *Comprehensive Organic Synthesis*, 2nd ed.; Molander, G.A., Knochel, P., Eds.; Elsevier: Oxford, UK, 2014; Volume 4, pp. 495–516.

46. Subramanian, H.; Landais, Y.; Sibi, M.P. Radical Addition Reactions. In *Comprehensive Organic Synthesis*, 2nd ed.; Molander, G.A., Knochel, P., Eds.; Elsevier: Oxford, UK, 2014; Volume 4, pp. 699–741.

47. Loertscher, B.M.; Castle, S.L. Radical Cyclizations and Sequential Radical Reactions. In *Comprehensive Organic Synthesis*, 2nd ed.; Molander, G.A., Knochel, P., Eds.; Elsevier: Oxford, UK, 2014; Volume 4, pp. 742–809.

48. Yoshioka, E.; Kohtani, S.; Jichu, T.; Fukazawa, T.; Nagai, T.; Takemoto, Y.; Miyabe, H. Direct Photoinduced Electron Transfer from Excited State of Rhodamine B for Carbon-Radical Generation. *Synlett* **2015**, *26*, 265–270. [CrossRef]

49. Majumdar, K.C.; Basu, P.K.; Chattopadhyay, S.K. Formation of five- and six-membered heterocyclic rings under radical cyclisation conditions. *Tetrahedron* **2007**, *63*, 793–826. [CrossRef]

50. Gansäuer, A. (Ed.) *Radicals in Synthesis I: Methods and Mechanisms*; Springer: Berlin, Germany, 2006.

51. Gansäuer, A. (Ed.) *Radicals in Synthesis II: Complex Molecules*; Springer: Berlin, Germany, 2006.

52. Taniguchi, T. Recent Advances in Reactions of Heteroatom-Centered Radicals. *Synthesis* **2017**, *49*, 3511–3534. [CrossRef]

53. Lynch, D.M.; Scanlan, E.M. Thiyl Radicals: Versatile Reactive Intermediates for Cyclization of Unsaturated Substrates. *Molecules* **2020**, *25*, 3094. [CrossRef]

54. Poater, J.; Viñas, C.; Bennour, I.; Escayola, S.; Solà, M.; Teixidor, F. Too Persistent to Give Up: Aromaticity in Boron Clusters Survives Radical Structural Changes. *J. Am. Chem. Soc.* **2020**, *142*, 9396–9407. [CrossRef]

55. Goulin, C.A.; Huber, T.A.; Nelson, J.M.; Macartney, D.H.; Baird, M.C. Atom Transfer Reactions Involving the Metal-centred Radical $[(\eta^5\text{-}C_5H_5)Cr(CO)_3]$. *J. Chem. Soc. Chem. Commun.* **1991**, 798–799. [CrossRef]

56. Gao, D.Z.; Liao, D.Z.; Jiang, Z.H.; Yan, S.P. Two hetero-spin metal–radical complexes exhibiting strong antiferromagnetic interactions between the metal ions and nitroxide radicals. *Transition Met. Chem.* **2008**, *33*, 107–112. [CrossRef]

57. Bai, W.; Li, L.; Fu, Y.; Tang, J.; Zhao, Y.; Wang, Y.; Li, Y. Radical metallacyclopropene: Synthesis, structure and aromaticity. *Dalton Trans.* **2023**, *52*, 9731–9736. [CrossRef]

58. Shao, X.; Wu, X.; Wu, S.; Zhu, C. Metal-Free Radical-Mediated C(sp3)-H Heteroarylation of Alkanes. *Org. Lett.* **2020**, *22*, 7450–7454. [CrossRef]

59. Ganesamoorthy, C.; Helling, C.; Wölper, C.; Frank, W.; Bill, E.; Cutsail, G.E., III; Schulz, S. From stable Sb- and Bi-centered radicals to a compound with a Ga=Sb double bond. *Nat. Commun.* **2018**, *9*, 87. [CrossRef]

60. Neidlinger, A.; Kienz, T.; Heinze, K. Spin Trapping of Carbon-Centered Ferrocenyl Radicals with Nitrosobenzene. *Organometallics* **2015**, *34*, 5310–5320. [CrossRef]

61. Yang, X.; Reijerse, E.J.; Nöthling, N.; SantaLucia, D.J.; Leutzsch, M.; Schnegg, A.; Cornella, J. Synthesis, Isolation, and Characterization of Two CationicOrganobismuth(II) Pincer Complexes Relevant in Radical RedoxChemistry. *J. Am. Chem. Soc.* **2023**, *145*, 5618–5623. [CrossRef] [PubMed]

62. Ke, J.; Lee, W.-C.C.; Wang, X.; Wang, Y.; Wen, X.; Zhang, X.P. Metalloradical Activation of In Situ-Generated α-Alkynyldiazomethanes for Asymmetric Radical Cyclopropanation of Alkenes. *J. Am. Chem. Soc.* **2022**, *144*, 2368–2378. [CrossRef] [PubMed]

63. Lee, W.-C.C.; Wang, D.-S.; Zhu, Y.; Zhang, X.P. Iron(III)-based metalloradical catalysis for asymmetric cyclopropanation via a stepwise radical mechanism. *Nat. Chem.* **2023**, *15*, 1569–1580. [CrossRef] [PubMed]

64. Xu, P.; Xie, J.; Wang, D.-S.; Zhang, X.P. Metalloradical approach for concurrent control in intermolecular radical allylic C−H amination. *Nat. Chem.* **2023**, *15*, 498–507. [CrossRef]

65. Shi, J.; Xu, W.; Yu, H.; Wang, X.; Jin, F.; Zhang, Q.; Zhang, H.; Peng, Q.; Abdurahman, A.; Wang, M. A Highly Luminescent Metallo-Supramolecular Radical Cage. *J. Am. Chem. Soc.* **2023**, *145*, 24081–24088. [CrossRef]

66. Frisch, M.J.; Trucks, G.W.; Schlegel, H.B.; Scuseria, G.E.; Robb, M.A.; Cheeseman, J.R.; Scalmani, G.; Barone, V.; Petersson, G.A.; Nakatsuji, H.; et al. *Gaussian 16. Revision B.01*; Gaussian, Inc.: Wallingford, CT, USA, 2016.

67. Hay, P.J.; Wadt, W.R. Ab initio effective core potentials for molecular calculations. Potentials for potassium to gold including the outermost core orbitals. *J. Chem. Phys.* **1985**, *82*, 299–310. [CrossRef]

68. Huzinaga, S. Basis sets for molecular calculations. *Comput. Phys. Rep.* **1985**, *2*, 281–339. [CrossRef]

69. Legault, C.Y. *CYLview, 1.0 b*; Université de Sherbrooke Sherbrooke: Sherbrooke, QC, Canada, 2009.

70. Schleyer, P.v.R.; Maerker, C.; Dransfeld, A.; Jiao, H.; Hommes, N.J.R.v.E. Nucleus-Independent Chemical Shifts: A Simple and Efficient Aromaticity Probe. *J. Am. Chem. Soc.* **1996**, *118*, 6317–6318. [CrossRef] [PubMed]

71. Szczepanik, D.W.; Andrzejak, M.; Dyduch, K.; Żak, E.; Makowski, M.; Mazur, G.; Mrozek, J. A uniform approach to the description of multicenter bonding. *Phys. Chem. Chem. Phys.* **2014**, *16*, 20514–20523. [CrossRef]

72. Szczepanik, D.W.; Andrzejak, M.; Dominikowska, J.; Pawełek, B.; Krygowski, T.M.; Szatylowicz, H.; Solà, M. The electron density of delocalized bonds (EDDB) applied for quantifying aromaticity. *Phys. Chem. Chem. Phys.* **2017**, *19*, 28970–28981. [CrossRef] [PubMed]

73. Lu, T.; Chen, F. Multiwfn: A multifunctional wavefunction analyzer. *J. Comput. Chem.* **2012**, *33*, 580–592. [CrossRef]

74. Schleyer, P.v.R.; Manoharan, M.; Wang, Z.X.; Kiran, B.; Jiao, H.; Puchta, R.; Hommes, N.J.R.v.E. Dissected nucleus-independent chemical shift analysis of pi-aromaticity and antiaromaticity. *Org. Lett.* **2001**, *3*, 2465–2468. [CrossRef] [PubMed]

75. Chen, Z.; Wannere, C.S.; Corminboeuf, C.; Puchta, R.; Schleyer, P.v.R. Nucleus-independent chemical shifts (NICS) as an aromaticity criterion. *Chem. Rev.* **2005**, *105*, 3842–3888. [CrossRef] [PubMed]

76. Fallah-Bagher-Shaidaei, H.; Wannere, C.S.; Corminboeuf, C.; Puchta, R.; Schleyer, P.V.R. Which NICS aromaticity index for planar π rings is best? *Org. Lett.* **2006**, *8*, 863–866. [CrossRef] [PubMed]

77. Gershoni-Poranne, R.; Stanger, A. The NICS-XY-scan: Identification of local and global ring currents in multi-ring systems. *Chem. Eur. J.* **2014**, *20*, 5673–5688. [CrossRef]

78.  Peeks, M.D.; Claridge, T.D.; Anderson, H.L. Aromatic and antiaromatic ring currents in a molecular nanoring. *Nature* **2017**, *541*, 200–203. [CrossRef] [PubMed]

79.  Sun, H.; An, K.; Zhu, J. Triplet State Aromaticity: NICS Criterion, Hyperconjugation, and Charge Effects. *Chem. Asian J.* **2016**, *11*, 234–240. [CrossRef] [PubMed]

80.  Herges, R.; Geuenich, D. Delocalization of electrons in molecules. *J. Phys. Chem. A* **2001**, *105*, 3214–3220. [CrossRef]

81.  Geuenich, D.; Hess, K.; Köhler, F.; Herges, R. Anisotropy of the induced current density (ACID), a general method to quantify and visualize electronic delocalization. *Chem. Rev.* **2005**, *105*, 3758–3772. [CrossRef]

82.  Zhu, Q.; Chen, S.; Chen, D.; Lin, L.; Xiao, K.; Zhao, L.; Solà, M.; Zhu, J. The application of aromaticity and antiaromaticity to reaction mechanisms. *Fundam. Res.* **2023**, *3*, 926–938. [CrossRef]

83.  Orozco-Ic, M.; Soriano-Agueda, L.; Escayola, S.; Sundholm, D.; Merino, G.; Matito, E. Understanding Aromaticity in [5] Helicene-Bridged Cyclophanes: A Comprehensive Study. *J. Org. Chem.* **2024**, *89*, 2459–2466. [CrossRef] [PubMed]